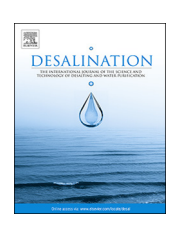
FISEVIER

Contents lists available at ScienceDirect

Desalination

journal homepage: www.elsevier.com/locate/desal



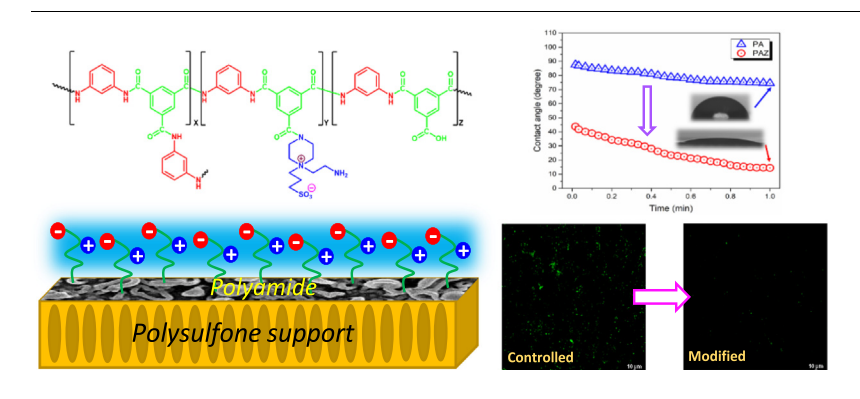
Zwitterionic forward osmosis membrane modified by fast second interfacial polymerization with enhanced antifouling and antimicrobial properties for produced water pretreatment



Yu-Hsuan Chiao^{a,d}, Shu-Ting Chen^a, Tanmoy Patra^b, Chen-Hua Hsu^d, Arijit Sengupta^a, Wei-Song Hung^{c,d,*}, Shu-Hsien Huang^d, Xianghong Qian^b, Ranil Wickramasinghe^{a,**}, Yung Chang^d, Kueir-Rarn Lee^d, Juin-Yih Lai^{c,d}

- ^a Department of Chemical Engineering, University of Arkansas, Fayetteville, AR 72701, United States
- ^b Department of Biomedical Engineering, University of Arkansas, Fayetteville, AR 72701, United States
- ^c Graduate Institute of Applied Science and Technology, National Taiwan University of Science and Technology, Taipei 10607, Taiwan
- d R&D Center for Membrane Technology, Department of Chemical Engineering, Chung Yuan University, Chung Li 32023, Taiwan

GRAPHICAL ABSTRACT



ARTICLE INFO

Keywords: Zwitterionic monomer Forward osmosis membrane Antifouling Second interfacial polymerization Antibacterial

ABSTRACT

In this work, superfast surface modification of forward osmosis (FO) membranes was accomplished using zwitterionic species with improved antibacterial and antifouling properties. Asymmetric thin film composite (TFC) FO membranes were fabricated using superfast second interfacial polymerization (SIP). The active sides of the TFC membranes were modified with zwitterionic polyamide moieties. Subsequently, the effects of surface modification on the surface properties, morphologies, and surface charges of the TFC membranes were investigated. The TFC membranes exhibited drastically improved performance in FO processes with model and real produced water samples. The zwitterion-augmentation significantly enhanced surface hydrophilicity and shielded negative surface charge distribution on the membrane surface. Furthermore, static protein absorption and dynamic protein fouling tests with model foulant sodium alginate (SA) revealed that the antifouling characteristics of the asymmetric TFC membranes had improved remarkably. SIP with zwitterion incorporation reduced protein absorption and promoted consistent flux during permeation with the model foulant solution. The antimicrobial characteristic of these FO membranes is also demonstrated with bacterial attachment on

E-mail addresses: wshung@mail.ntust.edu.tw (W.-S. Hung), swickram@uark.edu (R. Wickramasinghe).

^{*} Correspondence to: W.-S. Hung, Graduate Institute of Applied Science and Technology, National Taiwan University of Science and Technology, Taipei 10607, Taiwan.

^{**} Corresponding author.

membrane surface using *Escherichiacoli*. Overall, the zwitterion-augmented surface modification of these FO membranes resulted in enhanced permeability and reduction in surface structure parameter leading to improved antifouling properties with respect to organic proteins and gram-positive bacteria.

1. Introduction

Pretreatment of produced water comprised of complex organic molecules and surfactants has been a major challenge to tackle the surface and ground water pollution. Membrane-based separation is an energy-efficient, clean, environmentally benign, and easily commercially adaptable desalination or wastewater treatment technology that could help meet the increasing global demand for potable water [1-7]. The use of osmosis and distillation in desalination or wastewater treatment has been extensively studied [8]. However, the application of forward osmosis (FO) has been limited by membrane fouling and the task-specificity of FO membranes; thus, the fabrication of novel antifouling FO membranes with high efficiency warrants further investigation [9,10]. Although thin-film composite (TFC) asymmetric membranes demonstrate excellent performance when used as FO membranes [11,12], serious issues arise due to internal concentration polarization (ICP), which requires resolution [13,14]. Aromatic polyamide (PA) membranes are among the most common materials utilized in FO [15]. Nevertheless, these membranes suffer from extensive fouling during FO separation processes due to inherent structural and physicochemical properties. The extensive fouling is attributed to the rough surfaces of PA membranes which increase the surface areas available for foulant interaction. Several antifouling materials have been used to decorate the osmotic membrane for enhancing the antifouling property, such as MoS₂ [16], graphene oxide [7,17], TiO₂ [18], silver nanoparticle [11,19], hydrophilic polymer and monomer [20-24]. However, most of additives were modified by conventional in situ modification method which could change the structure of selective layer. Further, deprotonated -COOH acid groups on the surfaces of the membranes undergo electrostatic interactions with the metal ions present in feed solutions. Excessively large hydrophobic membrane surfaces induce hydrophobic interactions between membrane surfaces and nonpolar organic foulants in feed streams [25]. Moreover, most of these membranes are inadequate to treat complex produced water samples consisted of complex organic molecules, charged surfactants, etc. as foulant. Hence, significant efforts must be made towards development of a cost-efficient sustainable PA-based FO membranes to address these problems for commercial applications.

Zwitterionic monomers possess widely spread charge distribution in the form of constituent cationic and anionic moieties and thus provide free water hydration layers, enhanced water permeability [26], and drastically reduced fouling propensity [27-30]. Repulsive electrostatic interactions reduce the adsorption of positively or negatively charged foulants on membranes [31-34]. Our previous studies have demonstrated that zwitterion-augmented polysulfone (PSf) FO membranes fabricated through interfacial polymerization resulted in drastically improved water permeability and antifouling characteristics [20]. However, the anionic moieties of the zwitterions were exposed during interfacial polymerization which resulted led to structural changes in the selective layer. Ma et al. fabricated fouling-resistant reverse osmosis (RO) membranes introducing zwitterionic amine monomers on PSf supports which exhibited high water flux [35]. Moreover, the functionalization of membrane surface with these zwitterions also resulted in improved antimicrobial characteristics which are crucial for addressing biofouling and biofilm formation [31,36-38]. Zwitterion-augmented nanofiltration membranes also exhibited improved membrane permeability without compromised salt rejection. Hence, zwitterion augmentation was selected to improve the antifouling properties of the membranes with enhanced FO performance.

Although the reported literature studies have shown that the

introduction of zwitterionic moiety leads to excellent antifouling and antimicrobial properties, the modification time and maintaining intrinsic selectivity are important factor to be considered for commercialization. In previous FO membrane studies, the zwitterionic fragments were coated on the membrane *via* dopamine self-polymerization [39–41], but the self-polymerization reaction time required longer time scales of at least 1 h to 24 h. Atom transfer radical polymerization (ATRP) is also used to graft the zwitterionic brush on the polyamide layer, and the required reaction time is about 3 h after introduction of the initiator [19]. The second interfacial polymerization (SIP) provide a fast modification method within a couple minutes maintaining the structure of selective layer, which makes this process an important candidate for commercialization with significant cost minimization.

In this investigation, zwitterionic moieties were introduced during fabrication of asymmetric TFC FO membranes using SIP method. The fabrication of TFC FO membranes through conventional in situ chemical modification instead of SIP may result in the undesired modification of membrane surfaces in the intermediate state by subjecting the membranes to various chemicals. SIP incorporating polymers can decrease membrane permeability by increasing the overall membrane barrier thickness. Therefore, N-aminoethyl piperazine propane sulfonate (AEPPS), a zwitterionic monomer, was incorporated during the SIP of asymmetric TFC membranes. Modifications in surface properties were confirmed using detailed characterization methods. Further, improvements in FO performance due to zwitterionic incorporation were investigated using model as well as real produced water samples. The membranes were subjected to static and dynamic antifouling tests. The adsorption properties of proteins with negative and positive surface charges were studied in static mode. Fouling attributed to metal ions with different charges and organic molecules with different functional groups, such as SA, was also investigated in detail.

2. Material and methods

2.1. Materials

All the reagents used in this investigation were of ACS Reagent grade unless otherwise specified. Powdered Polysulfone (PSf) was provided by the R&D Center for Membrane Technology, CYCU (Chung Li, Taiwan). 1,3-Propanesultone (1,3-PS) was purchased from TCI (Portland, USA). 1,3,5-benzenetricarbonyl chloride (TMC), 1-Methyl-2-pyrrolidinone (NMP), and *n*-hexane were supplied by Fisher Scientific (Pittsburgh, PA). Phosphate-buffered saline (PBS) tablets, polyethylene glycol (PEG 200), SA, 1-(2-Aminoethyl) piperazine (AEP), acetonitrile, and *m*-phenylenediamine (MPD) were purchased from VWR (Atlanta, GA). Bovine serum albumin (BSA) was supplied by Lee BioSolution (Maryland Heights, MO). All inorganic salts (CaCl₂, NaCl, KH₂PO₄, MgSO₄, NaHCO₃, and NH₄Cl) and Lysozyme (LYZ) were procured from Sigma-Aldrich (St. Louis, MO). Sulfobetaine methacrylate (SBMA) used in this work was synthesized in the laboratory following literature reported procedure [42].

2.2. Fabrication of the TFC FO membranes

The zwitterionic species AEPPS was synthesized from AEP and 1,3-PS in acetonitrile medium in accordance with a previously reported method [20,43]. The solution of 1,3-PS solution was added dropwise into the AEP solution at a 1:1.1 M ratio at 60 $^{\circ}$ C and under continuous stirring. After 6 h of stirring, the yellow solid zwitterionic AEPPS was obtained and subsequently washed with acetonitrile to remove

unreacted precursors and side products. The resulting product was heated and dried at 30 °C using a vacuum oven.

The casting solution was prepared based on PSf content using 14 wt % PSf/NMP + 50 wt% PEG 200. A homogeneous solution was obtained by stirring the mixture for 12 h at 60 °C followed by cooling to room temperature without stirring to avoid the introduction of any air bubbles. The membrane support was fabricated following a generic nonsolvent induced phase separation process (NIPS). The precursor solution was spread on a clean glass plate (30 cm \times 25 cm) using a 120 μ m casting knife. The glass plate was promptly transferred into a coagulation bath of DI water maintained at 20 °C. Residual solvents were removed by frequently replacing the DI water in the bath. Finally, the fabricated PSf support was stored in a water bath in the dark until use.

The TFC FO membranes were fabricated through interfacial polymerization. The support membrane was cut into the appropriate dimensions and fixed on top of a clean glass plate. The custom PTFE frame was fixed on a glass plate by using four clips. Next, aqueous solution of 3 wt% MPD was poured into the frame and was left for 2 min on top of the membrane for surface deposition. A rubber roller was used to get rid of the excess aqueous solution from the surface of the membrane. The frame was clipped again, and the MPD-rich membrane was allowed to come in contact with 0.15 wt% TMC/hexane organic phase solution. After 1 min of reaction, the organic solution was drained from the frame. The support membrane was then subjected to interfacial polymerization. The resultant TFC membrane was annealed at 90 °C in a water bath for 2 min and subsequently, the fabricated PA membrane was stored in DI water for further investigation. In case of fabrication of PAZ, the surface modification process was like the PA membranes prior to the annealing step. SIP was performed thereafter by pouring 1 wt% AEPPS aqueous solution on top of the membrane surface to react with the surface -COOCl group. The reaction between the AEPPS solution and membrane was allowed to proceed for 1 min to induce the formation of a zwitterionic layer on the active sides of the TFC membranes. Subsequently, the unreacted AEPPS solution was decanted, and the membrane was annealed in a water bath for 2 min at 90 °C. The control and modified membranes were designated as PA and PAZ, respectively. The chemical structure of the resulting membrane is shown in Fig. 1.

2.3. Characterization of TFC FO membranes

All the membranes were washed with DI water and subsequently dried in vacuum chamber prior to characterization. The surface functionality of the membranes was analyzed using attenuated total reflectance-Fourier transform infrared spectroscopy (ATR-FTIR, Perkin Elmer Spectrum 100 FT-IR Spectrometer, Waltham, MA, USA). X-ray photoelectron spectrometry (XPS, Thermo Fisher Scientific Inc., Waltham, MA, USA) was conducted to characterize the chemical composition of the membranes. The water contact angle measurement instrument (model OCA15EC) used in this study was procured from Future Digital Scientific, Garden City, NY, USA. The atomic force microscope (AFM) utilized in this work was purchased from Bruker, CA. USA. The scanning electron microscope (SEM, FESEM S-4800) applied in this investigation was obtained from Hitachi Co., Tokyo, Japan. The zeta potential apparatus (SurPASS Electrokinetic Analyzer) was procured from Anton Paar, Ashland, VA, USA. These sets of equipment were used to characterize the surface charges, hydrophilicity, and morphology of the membranes. The bacterial attachment on the membrane surface was monitored using confocal microscopy (LSCM A1R), purchased from Nikon, Tokyo, Japan.

2.4. Performance of the TFC FO membranes

The water flux and reverse solute flux performances of the membranes were investigated in a cross-flow cell at room temperature (20 °C) by using a custom laboratory-scale apparatus manufactured by Membrane science Inc. The active area of the membrane used for the present investigation was $20\,\mathrm{cm}^2$. The co-current flow rate was fixed and controlled on both sides of the membrane by using a precise gear pump with a flow rate of $1\,\mathrm{L/min}$. A digital balance was used to measure flux on the basis of the permeated weight with an interval of $10\,\mathrm{min}$. A conductivity meter was applied to measure reverse solute flux by monitoring the change in the conductivity of the feed side with an interval of $10\,\mathrm{min}$. NaCl solutions with different concentrations were used as the draw solutions. A steady state was ensured prior to the collection of experimental data after $1\,\mathrm{h}$ of continuous operation. Two

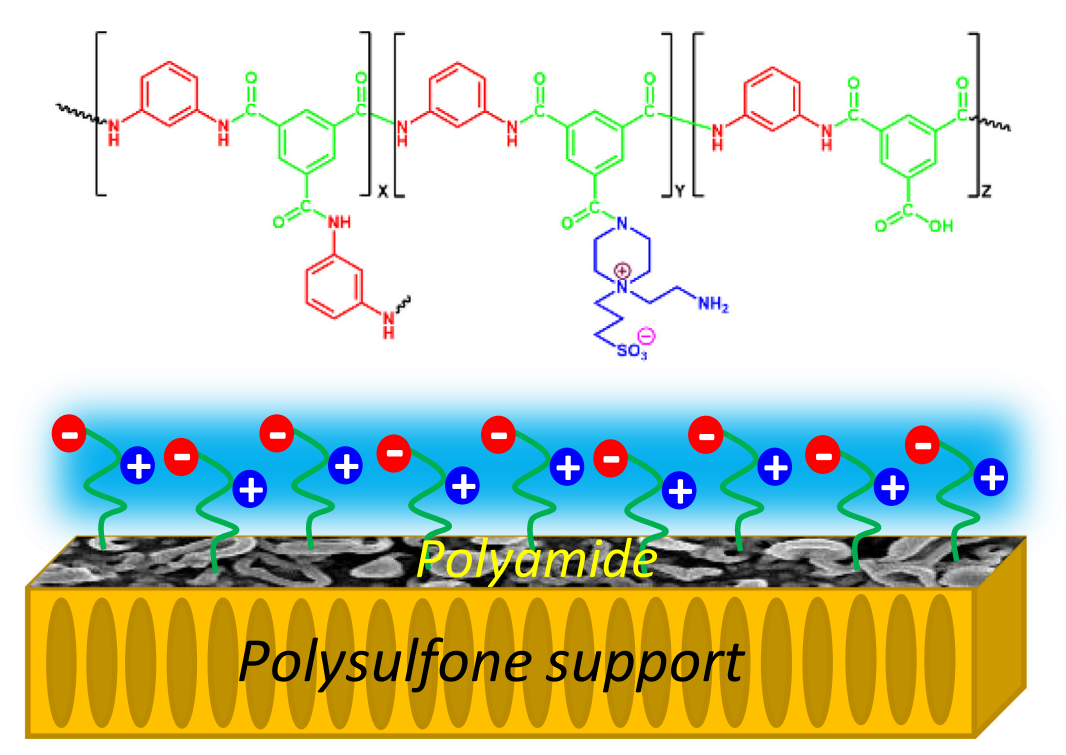


Fig. 1. Chemical structure of the resultant membrane after second interfacial polymerization.

liters of draw solution were used during the study to prevent draw solution dilution, which would affect the test. The related detailed measurement method and calculation theory are described in Eqs. (1) and (2) (SI. 1).

Intrinsic membrane properties, including pure water permeability A, solute permeability B, and solute rejection R, were evaluated using the custom-made laboratory-scale cross flow RO apparatus. The detailed description of the apparatus has been provided elsewhere [44]. The membranes were pre-compacted at 100 psi for 3 h to obtain a steady water flux. Furthermore, hydraulic pressure was reduced to 90 psi, and the flow rate was fixed at 0.6 LPM. Operation was carried out for at least 1 h prior to the collection of data from a digital balance. The structural parameter S was evaluated using a previously reported methodology described in SI. 2 Eq. (7) [45].

2.5. Bacterial attachment

The bacteria, Escherichia coli- Green fluorescent protein (E.coli GFP), was purchased from American Type Culture Collection (ATCC) and used to evaluate the antimicrobial behavior of TFC FO membrane. A medium comprised of 5.0 mg/mL peptone and 3.0 mg/mL beef extract was employed to culture the E.coli GFP. The culture medium was then incubated at 37 °C and subsequently shaken at 100 rpm for 12 h until a stationary state with final bacteria concentration of $10^6\,\text{cells/mL}$ was achieved. The membrane sample was washed with water and PBS buffer three times, respectively, and placed into the microplate. Further, the bacterial broth was added into the microplate for 5 h. After the adhesion test, the membrane was removed and rinsed with PBS buffer three times to remove the loosely adhering bio-foulants. The membrane sample was then positioned on the sample stage of a confocal microscope with the excitation and emission wavelength of 488 and 520 nm, respectively, to evaluate bacterial attachment level on the membrane surface.

2.6. Fouling properties of the TFC FO membranes

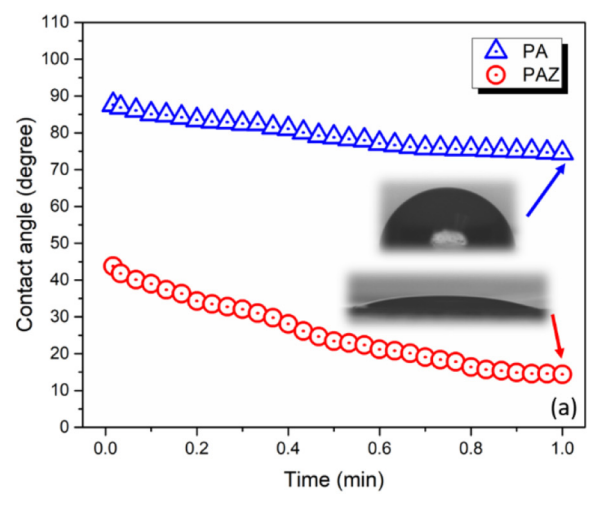
Static protein adsorption and dynamic fouling tests were conducted to understand the antifouling characteristics of the membranes. In the static adsorption test, the membrane was exposed to the positively charged protein LYZ and the negatively charged protein BSA in PBS buffer solution at pH7.4. Zwitterionic material can reduce fouling by positively or negatively charged foulants [46]. The PBS buffer solution was prepared by dissolving a PBS tablet in an appropriate volume of DI water. Next, 1 mg/mL BSA or LYZ protein was added to the PBS buffer. The membrane was cut into circular pieces with diameters of 2.54 cm.

Prior to immersion, the membranes were equilibrated through several rounds of rinsing with PBS buffer. The protein adsorption test was conducted for 24 h at room temperature and 60 rpm on a shaker. The protein content of the resultant solution was analyzed using UV–Visible spectroscopy by following any intensity change in the absorption peak at 280 nm. The absorption capacity of the membrane is described in SI 3.

Dynamic fouling is another method used to determine the antifouling properties of the membrane. The solution of SA was used as a model foulant for dynamic fouling test. SA solution (1 wt%) was stirred at 70 °C until a homogeneous mixture was obtained. The membrane was operated for 1 h with DI water on the feed side and 1 M NaCl solution on draw solution side, and the co-current cross flow rate for both sides was adjusted to 18.5 cm/s. Then, inorganic salts (0.5 mM CaCl₂, 9.2 mM NaCl, 0.45 mM KH₂PO₄, 0.61 mM MgSO₄, 0.5 mM NaHCO₃, and 0.93 mM NH₄Cl) were added to the 1 L feed tank, and the 2 L NaCl draw solution was adjusted to reach the initial flux of ~19.5 LMH. Next, SA concentration was adjusted to 250 ppm through the addition of 1 wt% SA solution. Data were recorded by using a balance with 10 min intervals until 500 mL of permeate had accumulated. The membrane was cleaned by replacing the feed solution with 15 mM NaCl [47]. Water flux through the clean membrane was measured by using the same process as that used to measure water flux before the addition of the SA foulant. The calculation of initial flux is described in Eq. (8) (SI. 3).

2.7. Fouling test with real produced water

Produced water samples were collected from APACHE (Houston, TX) and characterized in detail at the Arkansas Water Resources Center, University of Arkansas. The produced water composition was quantified in terms of dissolved inorganic materials, TDS, total suspended solids (TSS), and turbidity. Cationic and anionic composition were determined using Spectro Genesis ICP OES (Kleve, Germany) and Dionex DX-120 ion chromatograph (Sunnyvale, CA), respectively. EPA standard methods were employed to estimate the TDS and TSS to be 160.1 and 160.2 [43], respectively. Turbidity of the produced water samples were quantified using Turb 550 (WTW, Weilheim, Germany) turbiditymeter. TOC was estimated using a Skalar Formacs TOC analyzer (Breda, Netherlands). Percent difference between the sum of anions and cations in equivalent weight per liter was used to estimate the accuracy of the chemical analysis following the principle of electroneutrality.



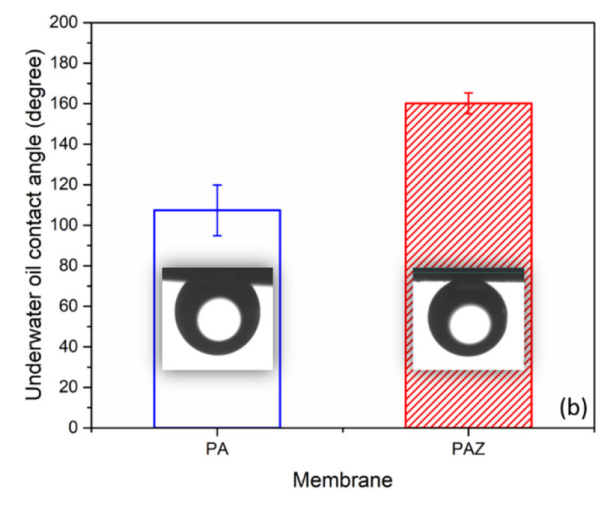


Fig. 2. Dynamic water contact angle (a) and underwater oil contact angle (b) of PA and PAZ.

3. Results and discussion

3.1. Physicochemical properties of the TFC FO membranes

Several techniques were used to characterize the surface properties of the zwitterionic TFC membranes in detail. The surface hydrophilicity of the TFC membranes was quantified through the water contact angle test with a sessile DI water droplet, as shown in Fig. 2a [48-50]. Wettability images were recorded after 1 min of water droplet residence on the membrane. The water contact angle test is a common and simple method for the identification of hydrophilicity and provides vital evidence for water permeability and antifouling phenomena. The PA layer has an average contact angle of ~80° within 1 min of water droplet residence time. The hydrophobic aromatic ring is responsible for the high contact angle of the PA layer. Air bubble entrapment between the water droplet and typical PA surface increased the water contact angle of the PA layer as previously reported by Elimelech et al. [15,51] The reaction of PAZ with hydrophilic zwitterionic moieties drastically decreased the water contact angle within 1 min to ~15°. This result demonstrates that a tightly bound hydrophilic water layer had formed on the PAZ surface. The zwitterionic moiety showed excellent oil/water separation performance because of the adequate hydrophilicity as reported in our earlier work [34], and sulfonic group-modified surfaces lead to formation of a strong hydration layer which enhances the antifouling properties [52]. In general, the introduction of superoleophobicity is characterized by the underwater oil contact angle of higher than 150°. The modified PAZ membrane showed significant increase in the underwater oil contact angle from ${\sim}110^{\circ}$ to ${\sim}160^{\circ}$ (Fig. 2b). Hence, it is evident from the contact angle measurement studies that the surface modification of the TFC FO membrane resulted in introduction of significant extent of superhydrophilicity and superoleophobicity.

The surface and cross-sectional SEM images of the membranes are shown in Fig. 3A-C and SI Fig. 2, respectively. The thicknesses of the two layers were negligibly different. The cross-sectional view reveals the presence of a thin (297 \pm 28 nm) PA layer on the support material overlaid by a marginally thicker (328 ± 34 nm) PAZ layer that resulted from the introduction of AEPPS into SIP. The surface view of the PA layer revealed that the nodule formation on PAZ had been mitigated. The surface roughness average (R₂) and root mean square roughness (R₀) of the layers was calculated and shown in Fig. 3d. The incorporation of the PA layer on the PSf support increased the root mean square and average roughness of the layers by almost 7-8-fold and increased the maximum roughness of the layers by 5-6-fold. The aromatic nature of the PA layer may be responsible for the increase in surface roughness. However, moderate reductions in roughness were observed after SIP. These observations are consistent with the observations gleaned from the AFM images presented in Fig. 3a-c.

ATR-FTIR was used to characterize the surface functionality of the modified membranes on the basis of the stretching/bending frequencies of the corresponding functional groups under excitation by IR light. Three new peaks representing amide 1 (C=O), amide 2 (NH), and amine (N-H) appeared in the spectra of PA and PAZ at 1680, 1543, and 1620 cm⁻¹, respectively [43,53,54]. Amide 1 corresponds to amide

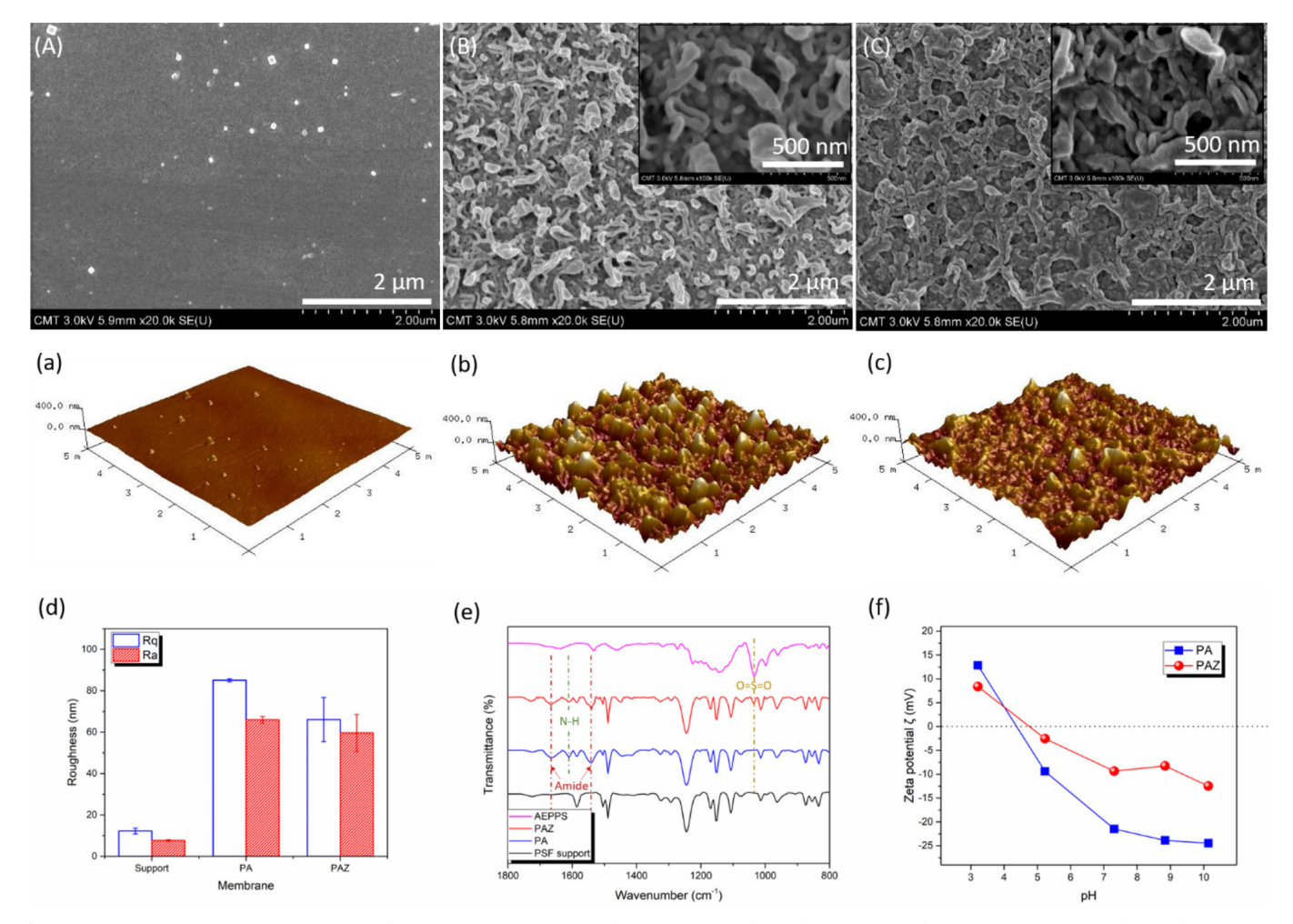


Fig. 3. SEM images of support (A), PA (B), and PAZ (C); 3D AFM images of support (a), PA (b), and PAZ (c); Roughness on support, PA, and PAZ (d); ATR-FTIR spectra of support, PA, and PAZ (e); zeta potential measurement data of PA and PAZ.

carbonyl, whereas amide 2 corresponds to amide N-H bonds. These peaks were ascribed to the PA layer, and their presence indicates that interfacial polymerization was successfully accomplished on the PSf support membrane. The peak at 1040 cm⁻¹ on PAZ corresponds to the sulfonate group (O=S=O) of the zwitterionic AEPPS monomer as previously reported and confirms that SIP was accomplished on the surface of the membrane [34]. Fig. 3e shows the FTIR spectra of the PSF support and other TFC membranes after first and second rounds of interfacial polymerization. The elemental compositions of the membranes were investigated through XPS analysis (SI Table 1). Elemental S in the support membrane was contributed by the PSf polymer, and the elemental N in PA and PAZ was attributed to the PA laver. S was not detected in PA because of the uniform deposition of the PA layer on the support [33]. This finding confirms that the support membrane had been successfully modified with a PA layer. Moreover, S contributed by the AEPPS monomer was detected in PAZ after SIP. FTIR and XPS results indicate that the PA membrane had formed on the support membrane and the AEPPS monomer was successfully grafted on the PA

The surface zeta potentials of PA and PAZ were investigated over a pH range of 3–10 as shown in Fig. 3f. At low pH values, the carboxylic acid groups of PA and PAZ were neutralized in presence of numerous H⁺ ions and the protonation of amine groups. Consequently, the overall surface charges of PA and PAZ became positive. In contrast, the zeta potential of PA and PAZ became negative at high pH values because of the deprotonation of —COOH groups and the formation of the anionic conjugated base —COO⁻ in the presence of numerous OH⁻ ions. The increase in the negative charges on PA may be attributed to the —COOH groups on the PA layer. The presence of the quaternary amine moieties of AEPPS increased the neutral charge and isoelectric point of PAZ. Therefore, the surface charge on PAZ membrane is significantly lower than that of PA membranes.

3.2. Performance of the TFC FO membrane

The FO performances of PA and PAZ in FO are shown in Fig. 4a–b. The concentration of the NaCl draw solution was adjusted to 1 or 2 M, and DI water was used as the feed solution. The water flux of PAZ increased by 65% (from 11.48 \pm 1.7 LMH to 18.91 \pm 1.46 LMH) and 47% (from 17.77 \pm 0.86 LMH to 26.17 \pm 1.03 LMH) when draw solutions of 1 and 2 M NaCl were used, respectively. Zwitterion incorporation enhanced the water permeability of PAZ. The occurrence of severe ICP with the use of 2 M draw solution mitigated the extent of enhancement in the water permeability of PAZ [13]. ICP must be resolved by optimizing the design of the support membrane. Increasing the salt concentration of the draw solution enhanced the reverse solute flux. In both draw solution concentrations, the reverse solute flux of PAZ was slightly higher than that of PA. Nevertheless, the reverse solute fluxes of the two membranes were similar. In addition, to optimize the

appropriate condition for grafting, the effect of various zwitterionic monomer concentrations (0–4 wt%) have been investigated and shown in SI Fig. 1. As the monomer concentration increased the water flux also increased. However, beyond the monomer concentration of 1 wt%, no significant alteration in water flux was observed. Thus, a monomer concentration of 1 wt% was chosen as the optimum parameter for further experimentations. Also, the PA and PAZ have similar specific flux (g/L) which means the cost of draw solution loss will not be increased after grafting the AEPPS on the surface instead of maintaining similar operation cost.

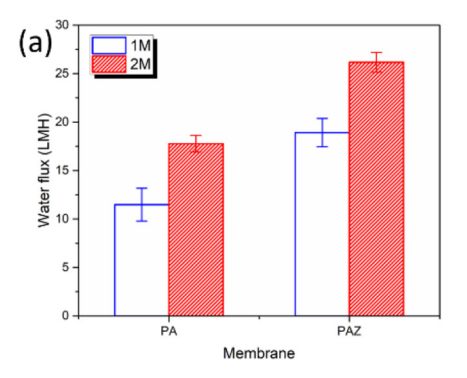
The A, B, and R of the membranes were quantified in RO mode. The results are presented in Fig. 4c PAZ had higher A (1.41 \pm 0.07 LMH/ bar) than PA (1.01 \pm 0.08 LMH/bar), and its B increased from 0.10 ± 0.004 LMH to 0.24 ± 0.022 LMH. The enhanced A of PAZ could be attributed to the increase in hydrophilicity contributed by the super hydrophilic zwitterionic moieties in AEPPS, which has a solubility close to that of water [55]. However, several studies have reported that A decreases after SIP [15,30] because the hydrophilic polymer may increase steric hindrance on the membrane surface and enhance water molecular resistance across the membrane [26]. Nevertheless, the R of PAZ remained constant (\sim 97%) even as its A increased. These phenomena demonstrate that SIP will not introduce defects to the original PA layer. As shown in Eq. (6) (SI. 2), the B of PAZ increased because B is related to R and A. S is a crucial index that describes ICP in FO [45]. The S value of PAZ was considerably lower than that of PA (S_{PA} = 0.99 $\,\pm\,$ 0.03 nm $\,S_{PAZ} = 0.56 \,\,\pm\,$ 0.01 mm) because the hydrophilic zwitterionic moieties of AEPPS increased the FO water flux.

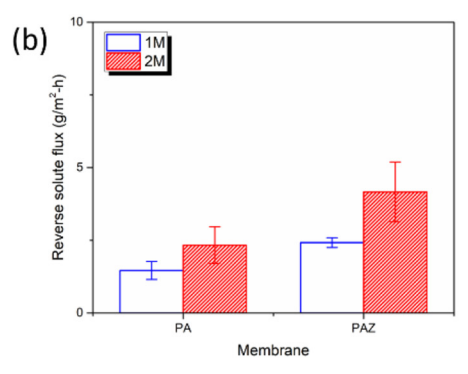
3.3. Bacterial attachment test

The antibacterial properties of membrane surface were evaluated using *E.coli* as a model biofoulant to challenge the active surface of TFC membrane in accordance with the previous literature [37,42,56]. Confocal microscopic images on bacterial adhesion on membrane surface are shown in Fig. 5a. The results were also compared with a model antifouling SBMA hydrogel standard (SI Fig. 3) which was detail described in our previous work [42,56,57]. The unmodified membrane PA (4810 cell/mm²) has very higher bacterial adhesion ability than zwitterionic modified membrane PAZ (352 cell/mm²) and the SBMA hydrogel standard sample (37 cell/mm²). The zwitterionic AEPPS effectively enhanced the antibacterial property of the modified membrane surface. This improvement was due to the smooth and superhydrophilic surface of the zwitterion incorporate FO membrane surface.

3.4. Antifouling characteristics of the TFC FO membranes

The antifouling properties of the resulting membranes in static and dynamic modes were investigated in detail. Antifouling property is an essential characteristic of membrane technology because severe fouling





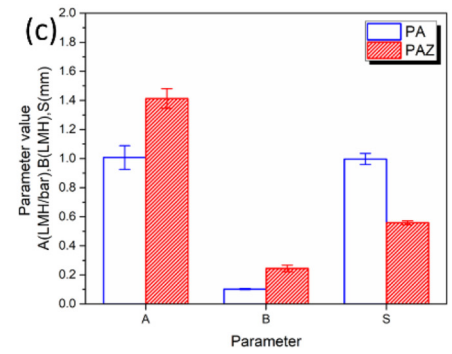


Fig. 4. Membrane performance of PA and PAZ in draw solutions with different salt concentrations: (a) water flux; (b) reverse solute flux on FO mode; (c) intrinsic membrane properties.

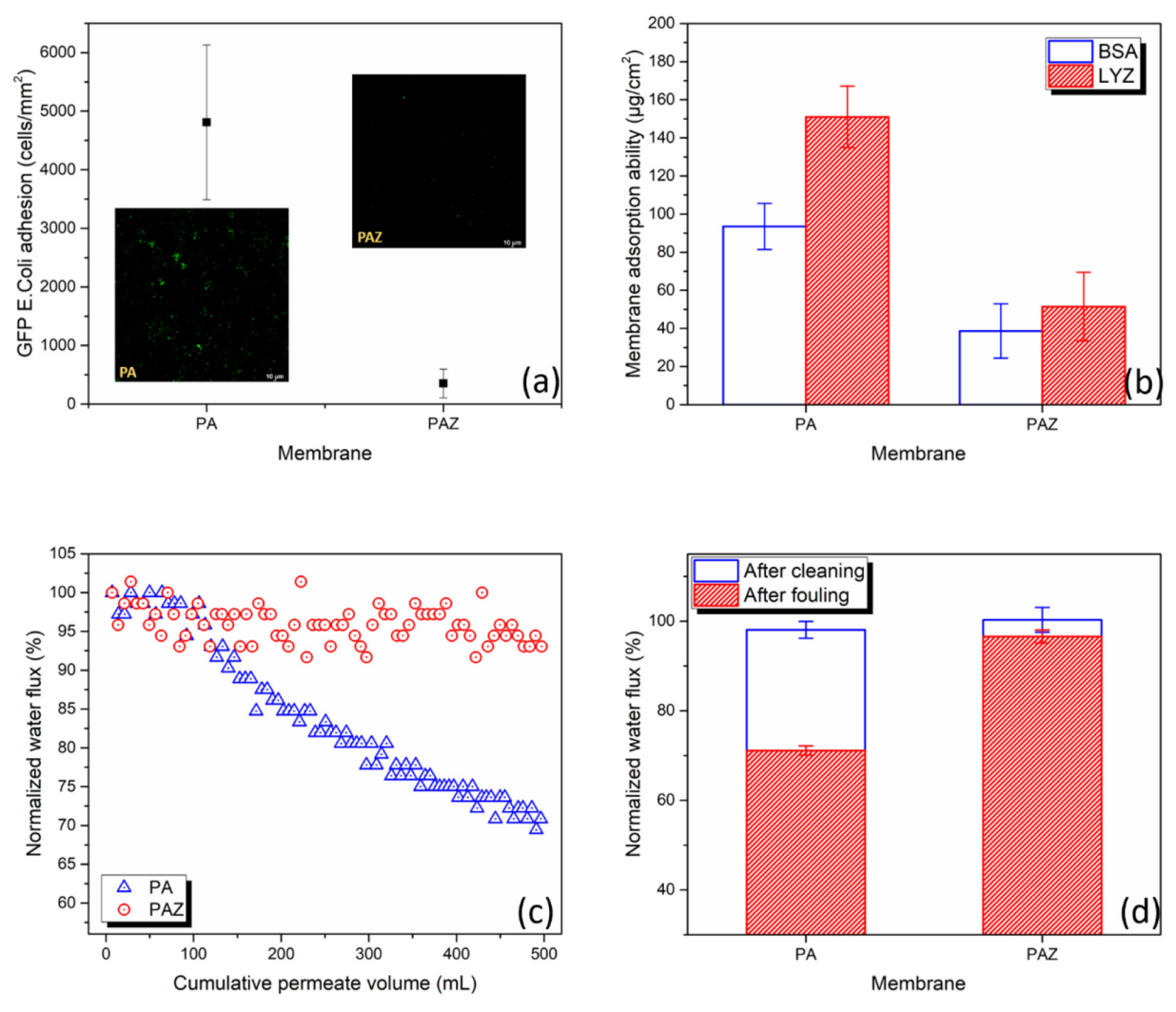


Fig. 5. Antibacterial and antifouling characteristics of TFC membranes: (a) Bacterial attachment experiment; (b) adsorption characteristics of charged proteins on membrane surfaces; (c) dynamic fouling test with a model foulant, initial flux is 19.5 LMH; (d) efficacy of the cleaning step.

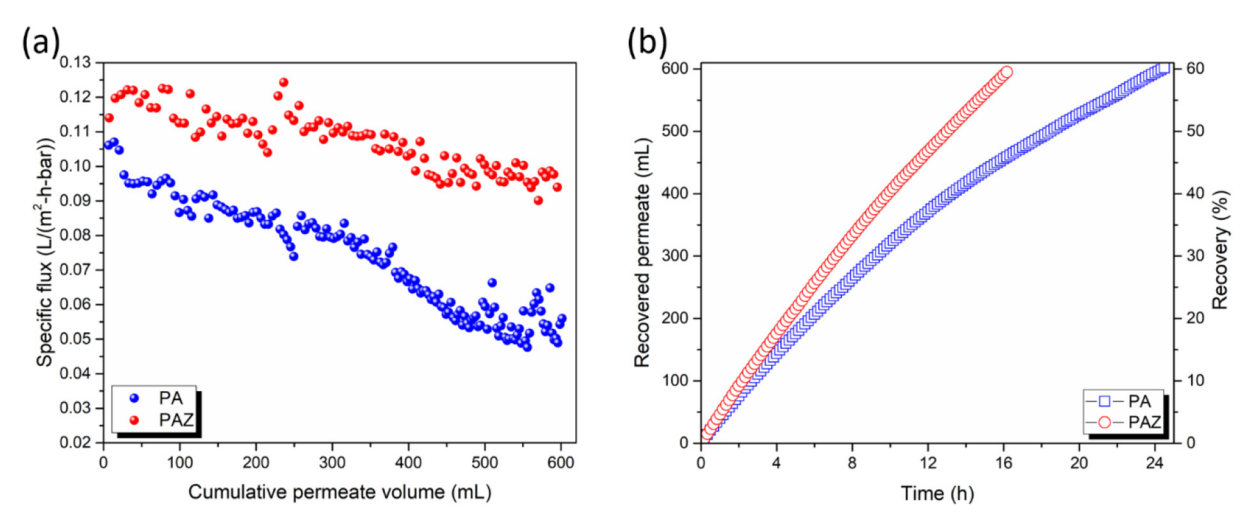


Fig. 6. Water flux measurement data for produced water sample, normalized water flux (a) and recoverability (b).

would degrade membrane performance and thus reduce operation lifetime. Reversible fouling on membrane surfaces can be reversed through a suitable cleaning procedure. Nevertheless, fouling may result in the irreversible and permanent deterioration of membrane performance. Thus, as shown in Fig. 5b–d PA and PAZ were subjected to static

protein adsorption and dynamic fouling tests. Previous studies have shown that the zwitterionic material can reduce the adsorption of positively and negatively charged foulants [29,37,38] and enhance water permeability [28,33,36]. In the static protein adsorption test (Fig. 5b), PA and PAZ were exposed to LYZ and BSA in PBS buffer solution at the

Property	Value	Property	Value
Total dissolved solids	47,783 ppm	Total nitrogen	8.3 ppm
Conductivity	66.2 mS/cm	Total phosphorus	0.01 ppm
Total suspended solids	7.2 ppm	Turbidity	20 NTU
Oil & Grease	461 ppm	рН	7.5

Fig. 7. Produced water analysis.

constant pH of 7.4. At pH 7.4, the surface charges of BSA and LYZ were -22.3 and $+3.5\,\text{mV}$ (Fig. 3f), respectively [31]. In accordance with the literature, the antifouling performance of PAZ was observed to be better than that of PA [55]. PA absorbed $93.52\,\mu\text{g/cm}^2$ BSA and $151\,\mu\text{g/cm}^2$ LYZ. PAZ absorbed $38.69\,\mu\text{g/cm}^2$ BSA and $51.48\,\mu\text{g/cm}^2$ LYZ. PA and PAZ showed lower adsorption ability for BSA than for LYZ. This characteristic was associated with the surface charge and roughness of the membranes. Real foulant protein adsorption ability should be lower than the results obtained in the present study because the actual membrane is an asymmetric TFC membrane that has a zwitterionic layer only on its active side. Therefore, PA and PAZ will inevitably encounter dynamic fouling test (Fig. 5c).

A model solution containing 0.45 mM KH₂PO₄, 9.20 mM NaCl, 0.61 mM, MgSO₄, 0.5 mM NaHCO₃, 0.5 mM CaCl₂, and 0.93 mM NH₄Cl and SA was used as the potential foulant because it contained monoand divalent inorganic ions, monovalent inorganic anions, and the organic foulant SA with multiple functional groups that may interact with the membrane surface. This model solution has also been used in dynamic membrane fouling tests in other works because SA can be used to simulate the polysaccharides present in city wastewater [43]. Especially, the bridging is easy to form between the alginate molecular and Ca²⁺ ions, and it will cause the alginate crosslink then to form the gellayer on the membrane surface. Consequently, the gel-layer may crash the stable driving force and lead to a low water flux. The drastic reduction in water flux over operation time was attributed to considerable membrane fouling [20]. Water flux through the PAZ membrane remained stable even after constant permeation with 500 mL (50% recovery) of the model solution. The baseline experiment was performed prior to the dynamic fouling experiment. These results demonstrate the substantial improvement in the antifouling characteristics of the membrane fabricated through SIP with zwitterionic modification. In accordance with previous studies [15,58], the normalized water flux of the PA or PAZ membrane could be restored to 100% after cleaning with 15 mM NaCl solution at 21 cm/s (Fig. 5d) [47]. Hence, in terms of performance the result confirms that a resilient FO membrane process was achieved using these modified membranes.

Produced water is a complex stream which contains oil and grease, high TDS, various surfactant organic chemical and so on [25,59-61]. With significant advancement in the horizontal drilling and hydraulic fracturing techniques, recycling the produced water is a big challenge in order to reduce the volume of water waste for economic benefits [62]. Herein, to investigate the commercial aspects of these TFC TO membranes, actual produced water samples were used to investigate the antifouling properties. Specific water flux $(L/(m^2-h-bar))$ measurement data using the produced water as feed the water analysis of produced water is shown in Fig. 7 4 M NaCl as draw solution, was calculated as $J_w/\pi;$ where J_w is the actual flux and π is the osmotic pressure of draw solution as shown in Fig. 6a. Minimized fouling effects were evident in case of PAZ as compared to PA with a reduced slope of flux decay. The experiment was run until accumulation of 600 mL permeate (~60% recovery). In case of PA membrane dramatic decline in specific water flux of ~52% was observed, in contrary to the gradual decrease of $\sim 20\%$ for PAZ membrane. The improved performance of the PAZ membrane can be mainly attributed to the enhanced antifouling properties of the membrane arising due to incorporation of zwitterionic moieties. Moreover, the recoverability data as shown in Fig. 6b, showed

that the PAZ membrane reached to almost 60% much faster within 16 h as compared to PA membrane which took almost 24 h. The faster recoverability can be attributed to higher water flux due to low antifouling property of the PAZ membrane. Overall, the PAZ membrane exhibited good separation performance against the real produced water samples obtained from Apache (Houston, TX) company. However, development of a sustainable operation process is another severe obstacle for the application of these membranes. Regeneration of the draw solution is considered to be an important parameter for FO processes. The combined FO-MD process has a huge potential to be a long-term solution for future commercial application of these membranes. It can combine both advantages (FO: low fouling, MD: high rejection) and mitigate both disadvantages (FO: the draw solution has to be regeneration, MD: severe fouling-fouling interaction between membrane and foulant) to build a low consumption produce water reuse plant [62].

4. Conclusions

In the scope of this study, asymmetric TFC FO membranes were fabricated from PSf support through superfast SIP processes involving PA followed by incorporation of zwitterionic moieties. Unlike conventional in situ modification, the SIP method used in this study was able to avoid the influence on the structure of the selective layer and additionally, promoted the antifouling and antibacterial properties. The zwitterionic surface modification was confirmed by ATR-FTIR spectroscopy and XPS. The surface morphology associated with the modification was investigated using SEM and AFM images. Electrostatic interaction between zwitterion incorporated membrane surfaces and water molecules significantly lowered the water contact angle from 80° to 15° and oil contact angle from 110° to 160° which in turn confirms the introduction of superoleophobicity. A significant reduction in the structural parameter from 1.06 mm to 0.66 mm was observed as evidenced by enhanced water flux and permeability. Moreover, the presence of zwitterionic moieties on the membrane surface substantially reduced the absorption of the negatively charged BSA and the positively charged LYZ. Dynamic fouling tests with the model foulant SA revealed that the permeability of the membranes remained constant during FO testing indicating significant improvement in antifouling characteristics of the membranes. The modified membrane showed ten times lower bacterial attachment than the unmodified membrane using E.coli. Overall, the fabricated zwitterion-augmented FO membranes exhibited improved performance in terms of water flux with lower membrane structure parameter and recoverability as compared to unmodified membranes with significantly improved antifouling and antibacterial properties. Combined FO-MD processes using these membranes have huge potential for commercial application for cost-effective pretreatment of surface as well as ground water for pollution reduction.

Acknowledgments

The authors gratefully acknowledge the financial support for this research extended by Membrane Science Inc. (Taiwan) through the NSF Industry/University Cooperative Research Center for Membrane Science, Engineering, and Technology; the National Science Foundation (IIP 1361809, 1822101, 1848682); and the University of Arkansas.

Appendix A. Supplementary data

Supplementary data to this article can be found online at https://doi.org/10.1016/j.desal.2019.114090.

References

 I. Alsvik, M.-B. Hägg, Pressure retarded osmosis and forward osmosis membranes: materials and methods, Polymers 5 (2013) 303–327.

[2] T.Y. Cath, A.E. Childress, M. Elimelech, Forward osmosis: principles, applications, and recent developments, J. Membr. Sci. 281 (2006) 70–87.

- [3] K. Smolders, A. Franken, Terminology for membrane distillation, Desalination 72 (1989) 249–262.
- [4] J.R. McCutcheon, R.L. McGinnis, M. Elimelech, Desalination by ammonia–carbon dioxide forward osmosis: influence of draw and feed solution concentrations on process performance, J. Membr. Sci. 278 (2006) 114–123.
- [5] G. Han, J.S. de Wit, T.-S. Chung, Water reclamation from emulsified oily wastewater via effective forward osmosis hollow fiber membranes under the PRO mode, Water Res. 81 (2015) 54–63.
- [6] S. Xiong, J. Zuo, Y.G. Ma, L. Liu, H. Wu, Y. Wang, Novel thin film composite forward osmosis membrane of enhanced water flux and anti-fouling property with N-[3-(trimethoxysilyl) propyl] ethylenediamine incorporated, J. Membr. Sci. 520 (2016) 400–414.
- [7] W.-S. Hung, T.-J. Lin, Y.-H. Chiao, A. Sengupta, Y.-C. Hsiao, S.R. Wickramasinghe, C.-C. Hu, K.-R. Lee, J.-Y. Lai, Graphene-induced tuning of the d-spacing of graphene oxide composite nanofiltration membranes for frictionless capillary action-induced enhancement of water permeability, J. Mater. Chem. A 6 (2018) 19445–19454.
- [8] T.-S. Chung, S. Zhang, K.Y. Wang, J. Su, M.M. Ling, Forward osmosis processes: yesterday, today and tomorrow, Desalination 287 (2012) 78–81.
- [9] W.C. Lay, J. Zhang, C. Tang, R. Wang, Y. Liu, A.G. Fane, Factors affecting flux performance of forward osmosis systems, J. Membr. Sci. 394 (2012) 151–168.
- [10] S. Lee, C. Boo, M. Elimelech, S. Hong, Comparison of fouling behavior in forward osmosis (FO) and reverse osmosis (RO), J. Membr. Sci. 365 (2010) 34–39.
- [11] A. Soroush, W. Ma, Y. Silvino, M.S. Rahaman, Surface modification of thin film composite forward osmosis membrane by silver-decorated graphene-oxide nanosheets, Environ. Sci. Nano 2 (2015) 395–405.
- [12] Y. Cui, X.-Y. Liu, T.-S. Chung, M. Weber, C. Staudt, C. Maletzko, Removal of organic micro-pollutants (phenol, aniline and nitrobenzene) via forward osmosis (FO) process: evaluation of FO as an alternative method to reverse osmosis (RO), Water Res. 91 (2016) 104–114.
- [13] C.Y. Tang, Q. She, W.C. Lay, R. Wang, A.G. Fane, Coupled effects of internal concentration polarization and fouling on flux behavior of forward osmosis membranes during humic acid filtration, J. Membr. Sci. 354 (2010) 123–133.
- [14] L. Huang, J.R. McCutcheon, Impact of support layer pore size on performance of thin film composite membranes for forward osmosis, J. Membr. Sci. 483 (2015) 25–33
- [15] X. Lu, S. Romero-Vargas Castrillón, D.L. Shaffer, J. Ma, M. Elimelech, In situ surface chemical modification of thin-film composite forward osmosis membranes for enhanced organic fouling resistance, Environ. Sci. Technol. 47 (2013) 12219–12228.
- [16] M.-N. Li, X.-F. Sun, L. Wang, S.-Y. Wang, M.Z. Afzal, C. Song, S.-G. Wang, Forward osmosis membranes modified with laminar MoS₂ nanosheet to improve desalination performance and antifouling properties, Desalination 436 (2018) 107–113.
- [17] L. Shen, S. Xiong, Y. Wang, Graphene oxide incorporated thin-film composite membranes for forward osmosis applications, Chem. Eng. Sci. 143 (2016) 194–205.
- [18] M. Ghanbari, D. Emadzadeh, W. Lau, T. Matsuura, M. Davoody, A. Ismail, Super hydrophilic TiO₂/HNT nanocomposites as a new approach for fabrication of high performance thin film nanocomposite membranes for FO application, Desalination 371 (2015) 104–114.
- [19] C. Liu, A.F. Faria, J. Ma, M. Elimelech, Mitigation of biofilm development on thinfilm composite membranes functionalized with zwitterionic polymers and silver nanoparticles, Environ. Sci. Technol. 51 (2016) 182–191.
- [20] Y.-H. Chiao, A. Sengupta, S.-T. Chen, S.-H. Huang, C.-C. Hu, W.-S. Hung, Y. Chang, X. Qian, S. Ranil Wickramasinghe, K.-R. Lee, J.-Y. Lai, Zwitterion augmented polyamide membrane for improved forward osmosis performance with significant antifouling characteristics, Sep. Purif. Technol. 212 (1) (2019) 316–325.
- [21] Y.-H. Chiao, A. Sengupta, S.-T. Chen, W.-S. Hung, J.-Y. Lai, L. Upadhyaya, X. Qian, S.R. Wickramasinghe, Novel thin-film composite forward osmosis membrane using polyethylenimine and its impact on membrane performance, Sep. Sci. Technol. (2019) 1–11.
- [22] Q. Yang, K.Y. Wang, T.-S. Chung, Dual-layer hollow fibers with enhanced flux as novel forward osmosis membranes for water production, Environ. Sci. Technol. 43 (2009) 2800–2805.
- [23] L. Shen, J. Zuo, Y. Wang, Tris (2-aminoethyl) amine in-situ modified thin-film composite membranes for forward osmosis applications, J. Membr. Sci. 537 (2017) 186–201.
- [24] L. Shen, X. Zhang, J. Zuo, Y. Wang, Performance enhancement of TFC FO membranes with polyethyleneimine modification and post-treatment, J. Membr. Sci. 534 (2017) 46–58.
- [25] Z. Anari, A. Sengupta, S. Wickramasinghe, Surface oxidation of ethylenechlorotrifluoroethylene (ECTFE) membrane for the treatment of real produced water by membrane distillation, Int. J. Environ. Res. Public Health 15 (2018) 1561.
- [26] S. Chen, L. Li, C. Zhao, J. Zheng, Surface hydration: principles and applications toward low-fouling/nonfouling biomaterials, Polymer 51 (2010) 5283–5293.
- [27] Z. Wang, J. Jin, D. Hou, S. Lin, Tailoring surface charge and wetting property for robust oil-fouling mitigation in membrane distillation, J. Membr. Sci. 516 (2016) 113–122.
- [28] Y.-C. Chiang, Y. Chang, C.-J. Chuang, R.-C. Ruaan, A facile zwitterionization in the interfacial modification of low bio-fouling nanofiltration membranes, J. Membr. Sci. 389 (2012) 76–82.
- [29] A. Venault, Y. Chang, Designs of zwitterionic interfaces and membranes, Langmuir 35 (2019) 1714–1726.
- [30] S.R.-V. Castrillón, X. Lu, D.L. Shaffer, M. Elimelech, Amine enrichment and poly (ethylene glycol)(PEG) surface modification of thin-film composite forward osmosis membranes for organic fouling control, J. Membr. Sci. 450 (2014) 331–339.
- [31] Y.-H. Zhao, X.-Y. Zhu, K.-H. Wee, R. Bai, Achieving highly effective non-biofouling

- performance for polypropylene membranes modified by UV-induced surface graft polymerization of two oppositely charged monomers, J. Phys. Chem. B 114 (2010) 2422–2429.
- [32] Q.-F. An, Y.-L. Ji, W.-S. Hung, K.-R. Lee, C.-J. Gao, AMOC positron annihilation study of zwitterionic nanofiltration membranes: correlation between fine structure and ultrahigh permeability, Macromolecules 46 (2013) 2228–2234.
- [33] Y.-F. Mi, Q. Zhao, Y.-L. Ji, Q.-F. An, C.-J. Gao, A novel route for surface zwitterionic functionalization of polyamide nanofiltration membranes with improved performance, J. Membr. Sci. 490 (2015) 311–320.
- [34] A. Venault, C.-Y. Chang, T.-C. Tsai, H.-Y. Chang, D. Bouyer, K.-R. Lee, Y. Chang, Surface zwitterionization of PVDF VIPS membranes for oil and water separation, J. Membr. Sci. 563 (1) (2018) 54–64.
- [35] J. Ma, Y. He, G. Zeng, X. Yang, X. Chen, L. Zhou, L. Peng, A. Sengupta, High-flux PVDF membrane incorporated with β-cyclodextrin modified halloysite nanotubes for dye rejection and Cu (II) removal from water, Polym. Adv. Technol. 29 (11) (2018) 2704–2714.
- [36] X.-D. Weng, Y.-L. Ji, R. Ma, F.-Y. Zhao, Q.-F. An, C.-J. Gao, Superhydrophilic and antibacterial zwitterionic polyamide nanofiltration membranes for antibiotics separation, J. Membr. Sci. 510 (2016) 122–130.
- [37] A. Venault, T.-C. Wei, H.-L. Shih, C.-C. Yeh, A. Chinnathambi, S.A. Alharbi, S. Carretier, P. Aimar, J.-Y. Lai, Y. Chang, Antifouling pseudo-zwitterionic poly (vinylidene fluoride) membranes with efficient mixed-charge surface grafting via glow dielectric barrier discharge plasma-induced copolymerization, J. Membr. Sci. 516 (2016) 13–25.
- [38] Z. Zhang, T. Chao, S. Chen, S. Jiang, Superlow fouling sulfobetaine and carboxybetaine polymers on glass slides, Langmuir 22 (2006) 10072–10077.
- [39] A. Nguyen, S. Azari, L. Zou, Coating zwitterionic amino acid l-DOPA to increase fouling resistance of forward osmosis membrane, Desalination 312 (2013) 82–87.
- [40] T. Cai, X. Li, C. Wan, T.-S. Chung, Zwitterionic polymers grafted poly (ether sulfone) hollow fiber membranes and their antifouling behaviors for osmotic power generation, J. Membr. Sci. 497 (2016) 142–152.
- [41] X. Zhang, J. Tian, S. Gao, W. Shi, Z. Zhang, F. Cui, S. Zhang, S. Guo, X. Yang, H. Xie, Surface functionalization of TFC FO membranes with zwitterionic polymers: improvement of antifouling and salt-responsive cleaning properties, J. Membr. Sci. 544 (2017) 368–377.
- [42] S.-H. Tang, M.Y. Domino, A. Venault, H.-T. Lin, C. Hsieh, A. Higuchi, A. Chinnathambi, S.A. Alharbi, L.L. Tayo, Y. Chang, Bioinert control of zwitterionic poly (ethylene terephtalate) fibrous membranes. Langmuir 35 (2019) 1727–1739.
- [43] R. Ma, Y.-L. Ji, X.-D. Weng, Q.-F. An, C.-J. Gao, High-flux and fouling-resistant reverse osmosis membrane prepared with incorporating zwitterionic amine monomers via interfacial polymerization, Desalination 381 (2016) 100–110.
- [44] M.B.M.Y. Ang, Y.-L. Ji, S.-H. Huang, H.-A. Tsai, W.-S. Hung, C.-C. Hu, K.-R. Lee, J.-Y. Lai, Incorporation of carboxylic monoamines into thin-film composite polyamide membranes to enhance nanofiltration performance, J. Membr. Sci. 539 (2017) 52–64.
- [45] T.Y. Cath, M. Elimelech, J.R. McCutcheon, R.L. McGinnis, A. Achilli, D. Anastasio, A.R. Brady, A.E. Childress, I.V. Farr, N.T. Hancock, J. Lampi, L.D. Nghiem, M. Xie, N.Y. Yip, Standard methodology for evaluating membrane performance in osmotically driven membrane processes, Desalination 312 (2013) 31–38.
- [46] M.-C. Sin, S.-H. Chen, Y. Chang, Hemocompatibility of zwitterionic interfaces and membranes, Polym. J. 46 (2014) 436.
- [47] B. Mi, M. Elimelech, Organic fouling of forward osmosis membranes: fouling reversibility and cleaning without chemical reagents, J. Membr. Sci. 348 (2010) 337–345.
- [48] H.H. Himstedt, A. Sengupta, X. Qian, S.R. Wickramasinghe, Magnetically responsive nano filtration membranes for treatment of coal bed methane produced water, J. Taiwan Inst. Chem. Eng. 94 (2019) 97–108.
- [49] M. Kamaz, P. Rocha, A. Sengupta, X. Qian, R.S. Wickramasinghe, Efficient removal of chemically toxic dyes using microorganism from activated sludge: understanding sorption mechanism, kinetics, and associated thermodynamics, Sep. Sci. Technol. (2018) 1–17.
- [50] M. Jebur, A. Sengupta, Y.-H. Chiao, M. Kamaz, X. Qian, R. Wickramasinghe, Pi electron cloud mediated separation of aromatics using supported ionic liquid (SIL) membrane having antibacterial activity, J. Membr. Sci. 556 (2018) 1–11.
- [51] A. Tiraferri, Y. Kang, E.P. Giannelis, M. Elimelech, Highly hydrophilic thin-film composite forward osmosis membranes functionalized with surface-tailored nanoparticles, ACS Appl. Mater. Interfaces 4 (2012) 5044–5053.
- [52] X. Zhang, J. Tian, S. Gao, Z. Zhang, F. Cui, C.Y. Tang, In situ surface modification of thin film composite forward osmosis membranes with sulfonated poly (arylene ether sulfone) for anti-fouling in emulsified oil/water separation, J. Membr. Sci. 527 (2017) 26–34.
- [53] B.M. Carter, A. Sengupta, X. Qian, M. Ulbricht, S.R. Wickramasinghe, Controlling external versus internal pore modification of ultrafiltration membranes using surface-initiated AGET-ATRP, J. Membr. Sci. 554 (2018) 109–116.
- [54] G. Song, A. Sengupta, X. Qian, S.R. Wickramasinghe, Investigation on suppression of fouling by magnetically responsive nanofiltration membranes, Sep. Purif. Technol. 205 (2018) 94–104.
- [55] X. Weng, Y. Ji, F. Zhao, Q. An, C. Gao, Tailoring the structure of polyamide thin film composite membrane with zwitterions to achieve high water permeability and antifouling property, RSC Adv. 5 (2015) 98730–98739.
- [56] Y. Chang, W.-J. Chang, Y.-J. Shih, T.-C. Wei, G.-H. Hsiue, Zwitterionic sulfobetaine-grafted poly(vinylidene fluoride) membrane with highly effective blood compatibility via atmospheric plasma-induced surface copolymerization, ACS Appl. Mater. Interfaces 3 (2011) 1228–1237.
- [57] Y. Chang, W. Yandi, W.-Y. Chen, Y.-J. Shih, C.-C. Yang, Y. Chang, Q.-D. Ling, A. Higuchi, Tunable bioadhesive copolymer hydrogels of thermoresponsive poly(N-

- isopropyl acrylamide) containing zwitterionic polysulfobetaine, Biomacromolecules 11 (2010) 1101–1110.
- [58] F.A. Siddiqui, Q. She, A.G. Fane, R.W. Field, Exploring the differences between forward osmosis and reverse osmosis fouling, J. Membr. Sci. 565 (2018) 241–253.
- [59] K. Sardari, P. Fyfe, D. Lincicome, S.R. Wickramasinghe, Aluminum electrocoagulation followed by forward osmosis for treating hydraulic fracturing produced waters, Desalination 428 (2018) 172–181.
- [60] M. Kamaz, A. Sengupta, A. Gutierrez, Y.-H. Chiao, R. Wickramasinghe, Surface modification of PVDF membranes for treating produced waters by direct contact
- membrane distillation, Int. J. Environ. Res. Public Health 16 (2019) 685.
- [61] C. Boo, J. Lee, M. Elimelech, Omniphobic polyvinylidene fluoride (PVDF) membrane for desalination of shale gas produced water by membrane distillation, Environ. Sci. Technol. 50 (2016) 12275–12282.
- [62] H. Chang, T. Li, B. Liu, R.D. Vidic, M. Elimelech, J.C. Crittenden, Potential and implemented membrane-based technologies for the treatment and reuse of flowback and produced water from shale gas and oil plays: a review, Desalination 455 (2019) 34–57.